Interdecadal Changes in El Niño Onset in the Last Four Decades

BIN WANG

Department of Meteorology, University of Hawaii, Honolulu, Hawaii

(Manuscript received 10 November 1993, in final form 17 June 1994)

ABSTRACT

The characteristics of the onset of the Pacific basin-wide warming have experienced notable changes since the late 1970s. The changes are caused by a concurrent change in the background state on which El Niño evolves.

For the most significant warm episodes before the late 1970s (1957, 1965, and 1972), the atmospheric anomalies in the onset phase (November to December of the year preceding the El Niño) were characterized by a giant anomalous cyclone over east Australia whose eastward movement brought anomalous westerlies into the western equatorial Pacific, causing development of the basin-wide warming. Meanwhile, the trades in the southeastern Pacific (20°S–0°, 125°–95°W) relaxed back to their weakest stage, resulting in a South American coastal warming, which led the central Pacific warming by about three seasons. Conversely, in the warm episodes after the late 1970s (1982, 1986–87, and 1991), the onset phase was characterized by an anomalous cyclone over the Philippine Sea whose intensification established anomalous westerlies in the western equatorial Pacific. Concurrently, the trades were enhanced in the southeastern Pacific, so that the coastal warming off Ecuador occurred after the central Pacific warming.

It is found that the atmospheric anomalies occurring in the onset phase are controlled by background SSTs that exhibit a significant secular variation. In the late 1970s, the tropical Pacific between 20°S and 20°N experienced an abrupt interdecadal warming, concurrent with a cooling in the extratropical North Pacific and South Pacific and a deepening of the Aleutian Low. The interdecadal change of the background state affected El Niño onset by altering the formation of the onset cyclone and equatorial westerly anomalies and through changing the trades in the southeast Pacific, which determine whether a South American coastal warming leads or follows the warming at the central equatorial Pacific.

1. Introduction

One of the fundamental questions concerning the nature and prediction of El Niño–Southern Oscillation (ENSO) is how the turnabout from a cold to a warm state (or vice versa) takes place. This question was originally raised by Bjerknes (1969) and has remained an outstanding issue to date (Cane 1993). A satisfactory answer to this question may also address other related important questions, such as what determines the preferred timescale and what causes the aperiodicity of the Southern Oscillation (SO), and why the transition between warm and cold states is intimately linked to annual cycles (Wyrtki 1982): The present analysis will focus on the transition from a cold to a warm state of the ENSO cycle.

Rasmusson and Carpenter (1982) made a comprehensive description of a composite ENSO scenario based on six events during 1950–1976. They found significant westerly anomalies occurring over the western equatorial Pacific in the onset (around the end of the year preceding El Niño) phase. These westerly anomalies occurring in the western equatorial Pacific can induce eastward propagating equatorial Kelvin waves and have been suggested as the trigger of the South American coastal warming (Wyrtki 1975; Philander 1981, 1985; Busalacchi and O'Brien 1981).

What is responsible for the initial changes in the western Pacific wind field? A variety of speculations have been made, including the twin cyclones that develop in the western-central Pacific (Keen 1982), the impacts of the cold surges from the Southeast Asia winter monsoon (Lau et al. 1983), the enhancement of the Australian summer monsoon (Hackert and Hastenrath 1986), and the persistent development of the intraseasonal oscillation (Lau and Chan 1986). In a series of studies, Barnett (1983, 1984, 1985) suggested that the surface wind and sea level pressure (SLP) anomalies, which eventually cause most of the changes in SST in the equatorial Pacific, originate in the equatorial Indian Ocean and propagate slowly eastward into the Pacific. The eastward propagation of free tropospheric zonal wind anomalies from the South Asian monsoon region to the western Pacific seen by Yasunari (1985, 1990) and Gutzler and Harrison (1987) seem to support Barnett's finding. An interpretation of the monsoon–ENSO connection was offered by Meehl

Corresponding author address: Prof. Bin Wang, Department of Meteorology, University of Hawaii at Manoa, 2525 Correa Road, HIG 331, Honolulu, HI 96822.

(1987), who emphasized the important impacts of the biennial variation of the monsoon circulation on ENSO. Trenberth and Shea's (1987) analysis of long record SLP data, on the other hand, revealed that the dominant feature of the SO is a standing seesaw, and the eastward propagation of SLP anomalies is not very regular and is not supported by the long-term record. They showed that changes over the South Pacific pole of the SO lead opposite changes in the Indonesian pole by one to two seasons. A possible South Pacific role in the ENSO onset was also discussed by van Loon and Shea (1985, 1987), Trenberth and Shea (1987), and Kiladis and van Loon (1988). The previous diverse and disputed views invite further investigations.

Three recent warm events (1982–83, 1986–87, 1991–92), which were documented by Gill and Rasmusson (1983), Kousky and Leetmaa (1989), Wang (1992), Janowiak (1993), and Kousky (1993), appear to behave quite differently from the canonical scenario of Rasmusson and Carpenter (1982) (RC composite hereafter). In the last three events the central Pacific warming was not preceded by South American coastal warming as described in RC composite. The change in the evolution of SST anomalies is not unique for the post-1950 period. Desser and Wallace (1987) noticed that the warming off Peru occurred in advance of the central Pacific warming (as inferred from the episode of positive Darwin SLP anomaly) in the 1925 event, whereas it occurred subsequent to the central Pacific warming in the 1930–31 and 1940–41 events. They, however, did not explore the causes for the change.

Because each warm event has its own character, case studies are necessary to reveal differences from case to case. The derived information is valuable for understanding the cause of the irregularities of the ENSO cycle. The present study is based on a case analysis of the six most significant events during 1950–1992. The intent is to document differences between the Rasmusson–Carpenter canonical ENSO scenario and the latest three ENSO events, and to reveal the causes of the differences. The results indicate that there have been remarkable changes in the characteristics of the onset after the 1976 warm event. The changes are attributed to an abrupt interdecadal change that occurred around 1977.

In this paper, the term El Niño is taken to be synonymous with a warm (or ENSO) episode, which means the major anomalous warmings of the eastern-central equatorial Pacific Ocean and along the coast of South America. Section 2 describes the data used in the present analysis. Following a brief discussion of the difference in the development of SST anomalies in section 3, a detailed documentation of the contrasting features of the atmospheric circulations and SST in the onset between pre-1977 and post-1977 events is given in section 4. Possible causes of the changes in the El Niño onset are discussed in section 5. The last section summarizes major results and discusses questions remaining open for future studies.

2. Data

The present analysis uses monthly mean SST, SLP, and surface winds derived from the Comprehensive Ocean–Atmosphere Data Sets (COADS) (Woodruff et al. 1987) of Monthly Summaries Trimmed (MST) format for the period from January 1950 to December 1992. Original COADS were on a 2° lat × 2° long grid. For the purpose of describing planetary-scale ENSO anomalies and making a more reliable estimation of monthly means, the 2° × 2° data were first combined into 5° lat × 15° long data by making observation-number-weighted box averages.

The analysis domain covers the tropical Indian and Pacific Oceans between 30°S and 30°N and from 40°E to 80°W. The monthly mean observations in each box, averaged for the period from January 1956 to December 1992, are more than 20 with the exception of five boxes located in the central equatorial Pacific and one box in the southeast Pacific where monthly mean observations are between 15 and 20 (Fig. 1a). The temporal distribution of observations at each box, averaged for the selected four locations (the western, central, eastern, and coastal equatorial Pacific), are given in Fig. 1b. The data density in the equatorial Pacific increased rapidly from 1955 to 1958, especially in the western and eastern equatorial Pacific. In the last three decades the frequency of observations in the equatorial Pacific has basically remained at the same level. In general, the data density appears to be adequate for case analyses of the significant ENSO events after 1957, but not for 1951 and 1953 episodes.

After obtaining the coarse-resolution data, further data quality control was performed. This included two steps. The first step was to check temporal consistency. For this purpose, annual cycle and monthly mean anomalies (MMA) were computed for each variable at each box. It was assumed that monthly mean values that were computed using more than 30 observations were "reliable." If observations were less than 15 per month and the difference between the MMA and its 3-month running mean exceeded two standard deviations of the MMA, or if the observation number was between 15 and 30 and the difference was higher than 1.5 standard deviation, the MMA under consideration was regarded as unreliable and removed. After the removal of all unreliable data, a temporal interpolation was used to make up the missing or deleted data in each box.

The second step of quality control was based on a spatial consistency principle. For the SST anomalies, the standard deviations of the spatial variability at a given time were computed for three different latitude bands: 10°S–10°N, 10°–20°S and 10°–20°N, 20°–30°S and 20°–30°N, respectively. The MMA at any

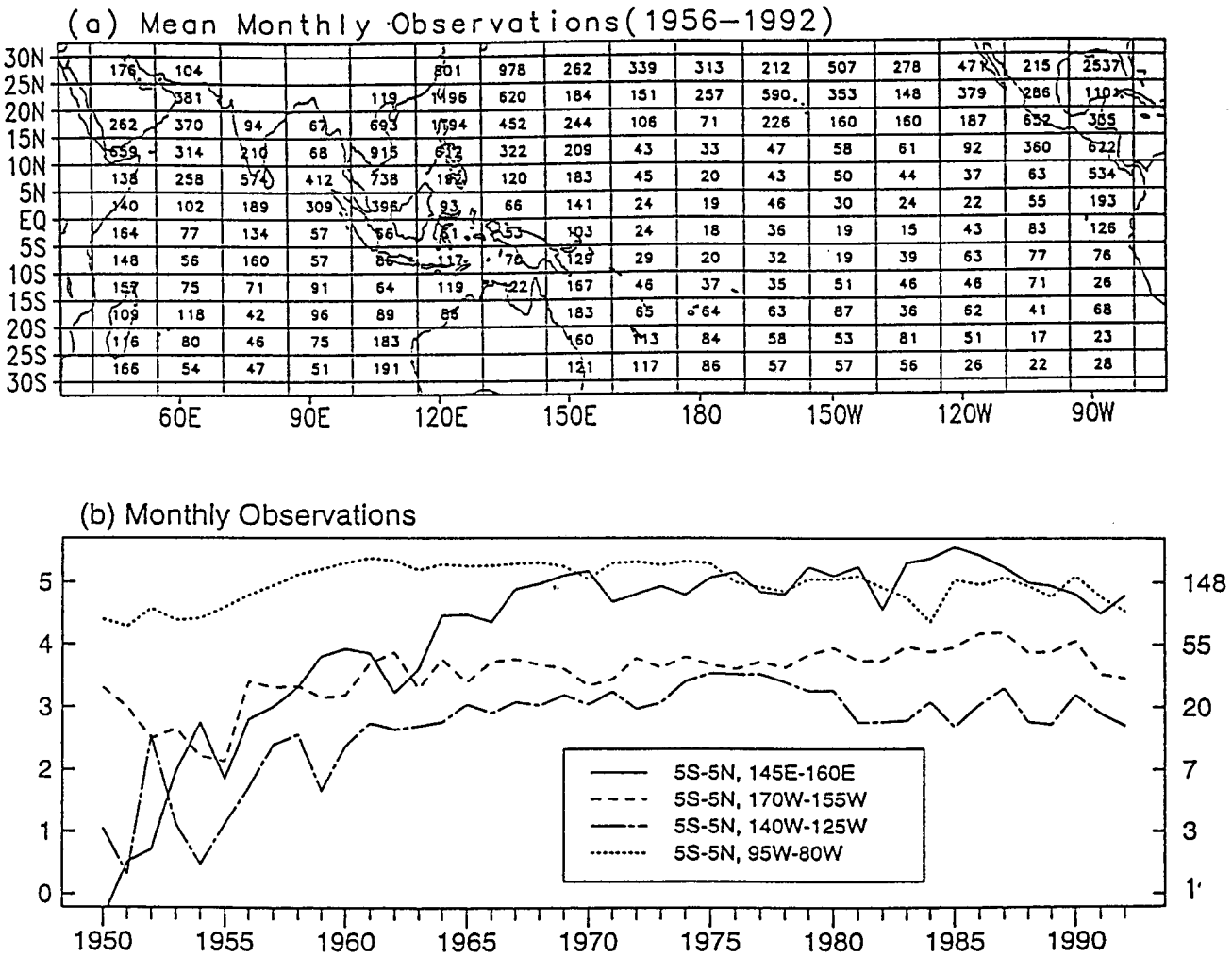

FIG. 1. (a) Monthly mean observations of COADS in each 5° lat × 15° long box averaged for the period January 1956–December 1992. (b) Temporal distribution of the monthly mean observations in each 5° × 15° box averaged, respectively, over the western (140°–150°E), central (170°–155°W), eastern (140°–125°W), and far eastern (95°–80°W) equatorial (5°S–5°N) Pacific. The number in the left (right) margin indicates natural logarithmic (actual) observational numbers per month.

box that exceeded the average of the corresponding four adjacent boxes by more than two standard deviations of the spatial variability were weeded out as unreliable if the corresponding monthly observation number was below 40. Such unreliable values were then replaced by the values obtained by a spatial interpolation scheme that combines Laplacian interpolation with cubic spline fitting. The SLP anomalies were checked using the same procedure except that 1.5 times the standard deviation was used as a criterion to check spatial consistency. For the zonal and meridional wind components, a value at a given box was regarded as unreliable if its sign was opposite to those of all four adjacent boxes and the observations were less than 40. The unreliable data were then replaced by spatially interpolated data. A nine-box weighted mean was used to smooth the anomalous SLP and wind component fields after the spatial interpolation. The weight was 0.72 for the central box, 0.06375 for the adjacent four boxes, and 0.0056 for the other four diagonal boxes.

The coarse resolution, though giving a more reliable estimation, reduces the amplitude of the anomalies.

3. Changes in the development of SST anomalies

For a Pacific basin-wide warming, the SST in the equatorial central Pacific (5°S–5°N, 170°–155°W) is a meaningful indicator for several reasons. First, it is derived from the best ship observations in the vast areas of the central and eastern Pacific (see shiplines 5 and 6 in Rasmusson and Carpenter 1982). Second, its variation reflects the SST variations in a large area of the equatorial eastern-central Pacific (5°S–5°N, 170°–95°W) (defined as El Niño Index) very well (Fig. 2).

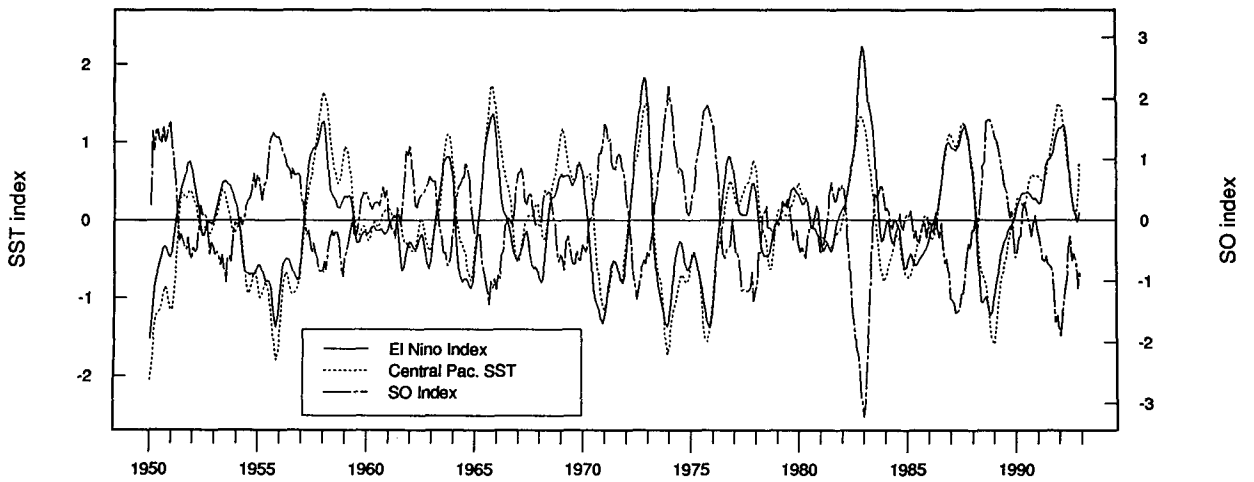

FIG. 2. Monthly mean SST anomaly (°C) at the central equatorial Pacific (5°S–5°N, 170°–155°W) (dotted), the El Niño index defined by the monthly mean SST anomaly (°C) averaged in the eastern-central equatorial Pacific (5°S–5°N, 95°–170°W) (solid), and the Southern Oscillation index defined by the monthly mean anomalous SLP difference (mb) between Tahiti and Darwin (Tahiti–Darwin) (dot–dashed). The data were low-pass filtered by a 5-month running mean with a weight (1:2:3:2:1).

It is also highly correlated with the SO index (Fig. 2). Last, the central Pacific has the largest equatorial east–west SST gradient and the anomalous warming there appears to be most influential to the shift of the rising branch of the Walker circulation and to the midlatitude circulation (Bjerknes 1966; Horel and Wallace 1981).

During 1950–1992 there were six most significant ENSO episodes (1957–58, 1965, 1972, 1982–83, 1986–87, and 1991–92) for which the El Niño Index exceeds one degree (Fig. 2). These episodes also contain warmings at both the South American coast and the central equatorial Pacific. There were three other moderate warm episodes (1963, 1969, and 1976–77), which not only have smaller amplitude (the El Niño Index is below one degree, Fig. 2) but also smaller spatial scale. These moderate episodes did not contain both a significant coastal and central Pacific warming (see Fig. 1 of Desser and Wallace 1990). For these moderate episodes it appears to be difficult to detect reliable signals because the signal-to-noise ratios are relatively low. For these reasons, only the six strongest episodes were selected for the case and composite studies.

The six strong basin-wide warm episodes have displayed different evolution of SST anomalies. This is evident from the comparison of the relative timing of the warming that occurred in the central Pacific and the far eastern Pacific (Fig. 3). In the equatorial central Pacific (5°S–5°N, 170°–155°W) the monthly mean SST is dominated by an interannual variation: The interannual variation carries 82%, whereas the annual cycle carries only less than 10% of the total variance. The annual cycle is skewed with a rapid increase from February to May by about 1°C. For the six strong episodes, the SST anomalies are maximum toward the end of the El Niño year except for the 1986–87 episode, which has double peaks with the major one occurring in the northern summer 1987 (Fig. 3a). Appreciable positive SST anomalies that are greater than 0.2°C normally occur from March to June of year 0 except during the 1991 event, which developed, unusually, from an above-normal state. The occurrence of positive SST anomalies tends to be in phase with the annual warming.

In the far eastern Pacific south of the equator (0°–5°S, 80°–95°W), the annual range of SST is large (about 4.5°C). The interannual variation is also pronounced (Fig. 3b). The peak anomalous warming occurred around June of year 0 in three pre-1977 warm episodes, while around April of year +1 in the post-1977 episodes. The peak annual warming at the same location occurs in March. Therefore, the pre-1977 episodes extended the annual peak warming in year 0, whereas the post-1977 episodes extended and amplified the annual peak warming in year +1. Note also that the pre-1977 episodes started around January and appeared as an amplification of the annual warming in year 0, whereas the post-1977 episodes started around July and appeared as a disappearance of the annual cooling in year 0.

Figure 3 indicates two notable differences in the evolution of SST anomalies between the pre- and post-1977 warm episodes. First, the eastern Pacific peak warming leads the central Pacific peak warming by about 5 months in three pre-1977 warm episodes, while lagging the central Pacific peak warming by about 5 months in the post-1977 warm episodes. In the pre-1977 cases the eastern Pacific warming can be used as a predictor to forecast the winter circulation anomalies in Northern Hemisphere extratropics at a lead of two seasons. Yet, the same predictor for the post-1977 period is not available and the prediction is apparently much more challenging. Second, in the central Pacific

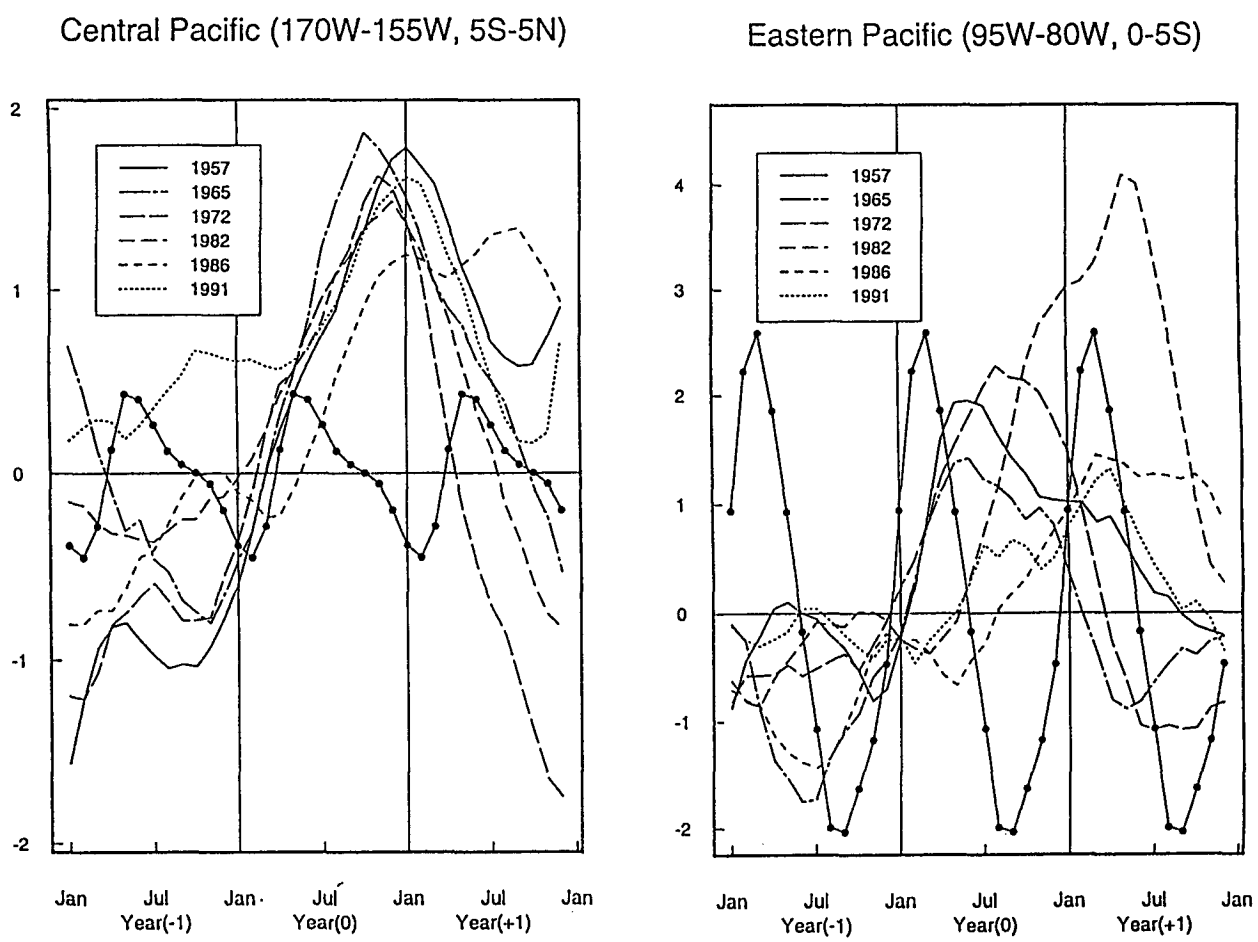

FIG. 3. Five-month weighted running mean SST anomalies (°C) for the six most significant warm events at the central equatorial Pacific (5°S–5°N, 170°–155°W) (left panel) and at the far eastern equatorial Pacific (0°–5°S, 95°–80°W) (right panel). The line with solids denotes annual cycles. The year 0 refers to the El Niño year in which anomalously high SST first appears and then amplifies in the tropical Pacific; year −1 and year +1 refer to the previous and subsequent years, respectively.

and during boreal fall of year −1, the pre-1977 episodes were preceded by a cooling of about 1°C, while the post-1977 episodes were near or above normal.

Based on a composite scenario derived from six warm episodes that occurred during 1950–1976, Rasmusson and Carpenter (1982) defined five phases for a warm episode: antecedent (June–October of year −1), onset (November of year −1 to January of year 0), peak (March–May of year 0), transition (June–October of year 0), and mature (November of year 0 to February of year +1). They named March–May of year 0 as the peak phase because the South American coast reaches its peak warming during that period for the pre-1977 episodes. In view of the fact that there was no obvious coastal warming prior to the central Pacific peak warming (mature phase) in the latest three episodes, the boreal spring of year 0 will be called a *development* phase. All other terminologies (antecedent, onset, transition, and mature) will follow Rasmusson and Carpenter (1982).

4. Contrasts in the onset between the pre- and post-1977 warm episodes

The evolution of SST anomalies during warm episodes, as seen from Figs. 3a,b, suggests a notable change in the evolution of El Niño after 1977. To understand the causes of the change, let us carefully examine the evolutions of the atmospheric fields, particularly around the onset phase.

a. SLP and surface wind anomalies

Seven-month running mean anomalies of surface winds and SLP were used for a case analysis of each of the six strong warm episodes. During the onset phase, the pre- (or post-) 1977 warm episodes bear similarities (Figs. 4a,b). For instance, in the southeast Pacific and South Indian Oceans anomalous westerlies prevail during the onset phase of the three pre-1977 episodes, whereas anomalous easterlies prevail during the three post-1977 episodes. Over the western Pacific and mar-

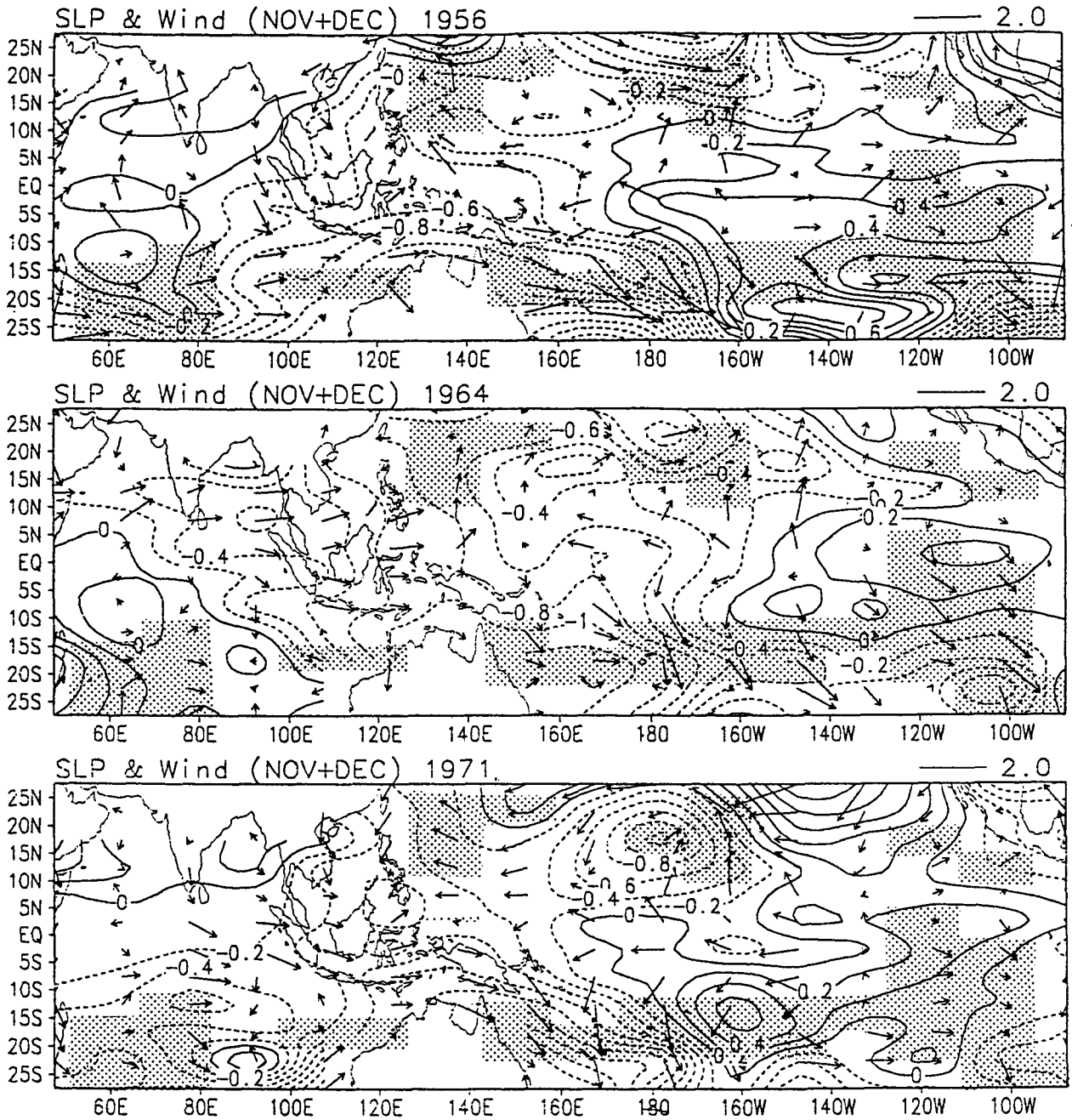

FIG. 4. Seven-month running mean anomalies of SLP and surface winds at the onset phase (November to December of year −1) for (a) the three pre-1977 events (1957, 1965, and 1972), and (b) the three post-1977 events (1982, 1986–87, 1991). The areas where the anomalous surface winds between the pre- and post-1977 composites differ significantly at the confidence level of 0.05 are shaded.

itime continent, anomalous equatorial westerlies tend to be associated with the negative SLP anomalies in Australia during the onset phase of the three pre-1977 episodes.

Note that the similarity among three post-1977 episodes is not as great as that among the pre-1977 episodes. This is partially attributed to the fact that the 1986–87 episode is not well phase-locked with the annual cycle. The mature phase of the ENSO normally occurs around November and December of year 0. This is true for all significant episodes considered in this study except the 1986–87 episode (Fig. 3a), which matured in the summer of year 0. The present composite is constructed according to calendar months. This approach is valid only if the evolution of the warm episodes is phase-locked with annual cycle. An alternative

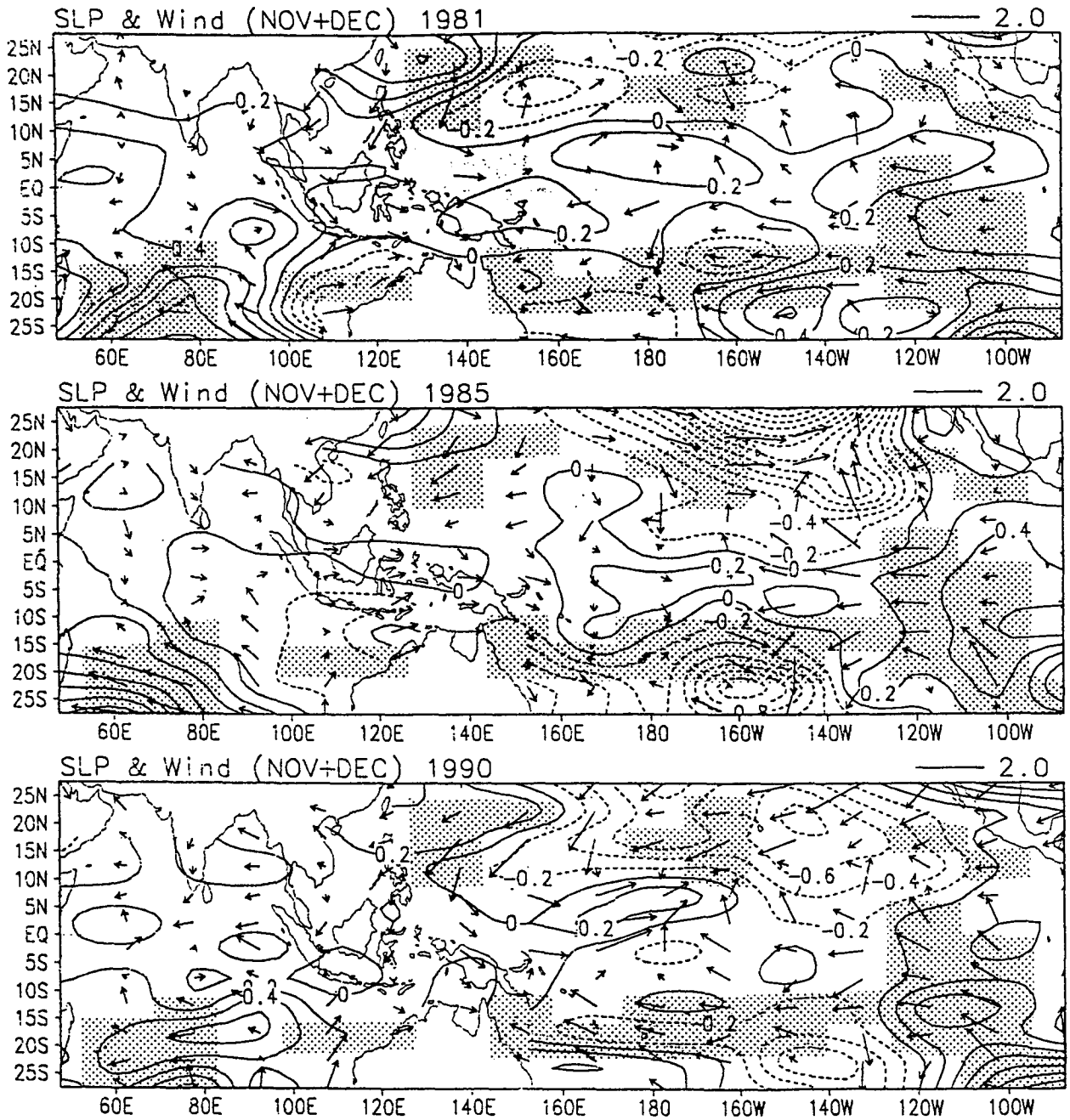

FIG. 4. (*Continued*)

way of making a composite is based on the phase of ENSO cycle. With the latter approach, the onset phase should be about 12 months in advance of the mature phase (i.e., in November and December of year −1). For those episodes that are tightly phase-locked with the annual cycle (the 1957, 1965, 1972, 1982, and 1991 episodes), the onset phases determined by the two approaches are nearly the same. For the exceptional 1986–87 episode, however, the onset phase should be in May and June 1986 if the composite is made according to the ENSO cycle itself. Figure 5 shows anomalous winds and SLP in May–June 1986. In the western Pacific, equatorial westerly anomalies are associated with an anomalous cyclone over the Philippine sea. This feature resembles the anomalous winds in the onset phases of the other two post-1977 episodes. With either composite approach, the similarities among the members within each group (the pre- and post-1977

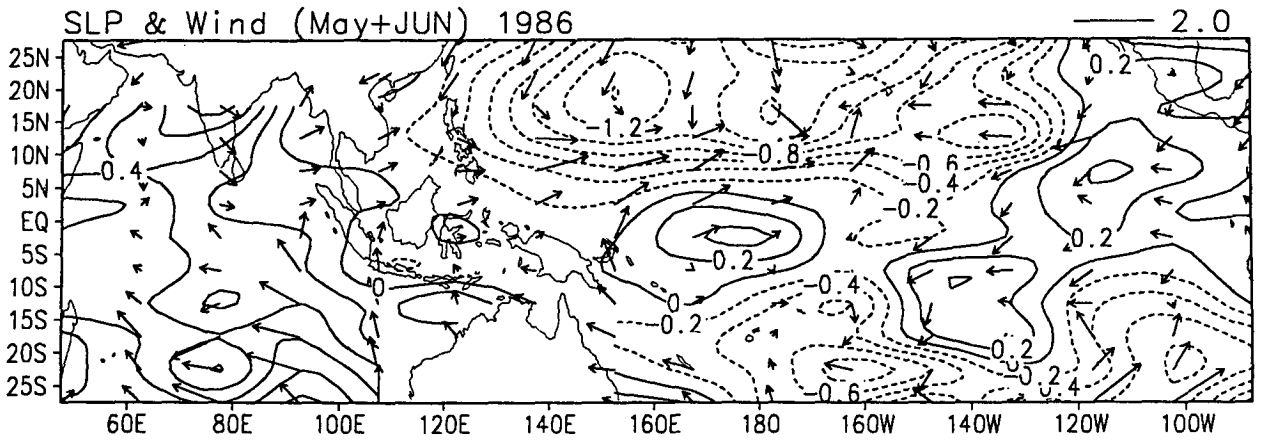

FIG. 5. Seven-month running mean anomalies of SLP and surface winds averaged for the period May–June 1986.

groups) are sufficient to warrant a meaningful composite.

The differences between two groups are apparently much larger than the differences among the members of each group. An F-test has been performed to determine the areas where the differences between the two composite wind fields are statistically significant at the 95% confidence level. These areas were illustrated in Figs. 4a,b by the shadings. In what follows, the discussion will focus only on those features that differ significantly for the pre- and post-1977 composites. Two sets of composite SLP and wind anomalies at four phases were made for the pre- and post-1977 episodes, respectively (Figs. 6 and 7).

In the antecedent and onset phases, the composite anomalous SLP for the pre-1977 warm episodes resembles a high-index state of the SO (Figs. 6a and 6b). The wind anomalies are dynamically consistent with the SLP anomalies, diverging in the eastern-central equatorial Pacific around 140°W. Significant easterly anomalies prevail over the central and western equatorial Pacific and westerly anomalies over the eastern Indian Ocean and the Maritime Continent, representing an enhanced Walker circulation. Conversely, the composite SLP anomalies in the anticedent phase for the post-1977 episodes are small (Fig. 7a) and bear some resemblance to a low-index state of the SO in the onset phase (Fig. 7b). The winds in the central Pacific and the equatorial Indian Ocean–Australian summer monsoon region are nearly normal in the onset phase, suggesting that the post-1977 episodes developed from a near-neutral condition.

A pronounced contrasting feature in the wind fields can be identified in the southeast trades. In the cases of the pre-1977 episodes, there is a persistent weakening of the trades in the southeast Pacific (95°–140°W) from the antecedent to development phase (Figs. 6a–c). In sharp contrast, for the post-1977 episodes, there is a persistent strengthening of the trades in the same region and the same period (Figs. 7a–c). The weakening (strengthening) of the southeast trades over the open ocean may favor (prohibit) warming occurring along the South American coast at the onset phase. One should also note that near the South American coast (80°–95°W) there is little difference in the surface wind fields between the two composites from the antecedent to development phase.

Another different feature is associated with the process of the establishment of equatorial westerly anomalies in the western Pacific. In the antecedent and onset phases of the pre-1977 episodes, pronounced westerly anomalies are found from the equatorial Indian Ocean across the Australian summer monsoon region to the South Pacific convergence zone (SPCZ) (Figs. 6a,b). These anomalous westerlies are associated with a giant anomalous low pressure and a cyclonic gyre centered in Australia in the antecedent phase and east of Australia in the onset phase. Pronounced negative pressure anomalies also occur along and southwest of the SPCZ. The cyclone and associated westerly anomalies move slowly eastward from the antecedent to onset phase as the easterly anomalies over the central and western Pacific decrease. The establishment of the equatorial westerly anomalies in the far western Pacific, thereby, appears to be associated with the eastward migration of the anomalous *Australian onset cyclone.* The latter represents an enhanced Australian summer monsoon. It is thus speculated that an enhanced Australian summer monsoon may have significant impacts on establishment of the westerly anomalies in the equatorial western Pacific for the pre-1977 episodes. To some extent, the above features are consistent with the results presented in previous studies that emphasized the roles of the variations in the South Pacific in the ENSO onset (Rasmusson and Carpenter 1982; van Loon and Shea 1985; Hackert and Hastenrath 1986; Trenberth and Shea 1987).

In the antecedent and onset phases of the post-1977 episodes (Figs. 7a,b), on the other hand, significant westerly anomalies occur in the western Pacific north

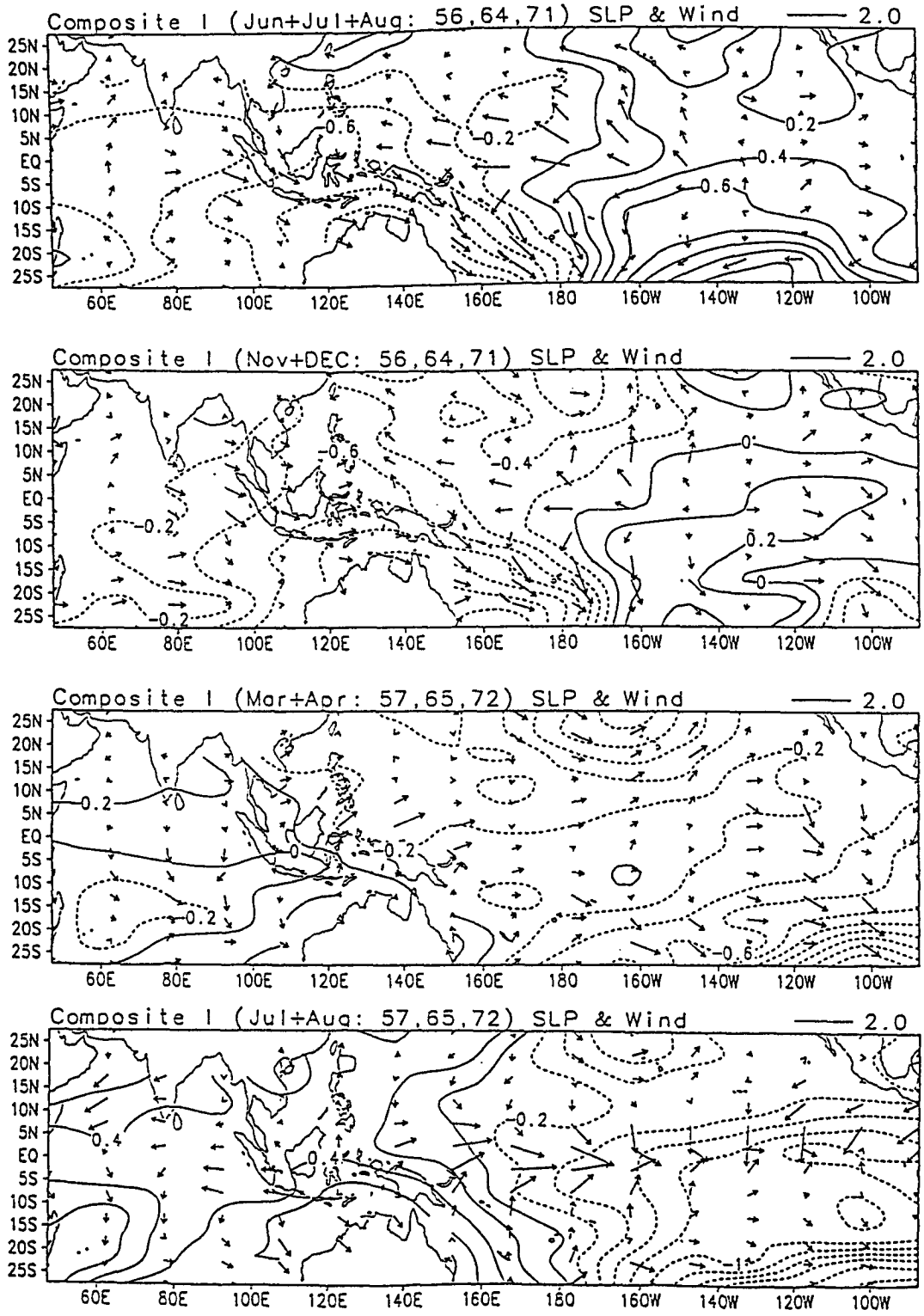

FIG. 6. Composite monthly mean anomalies (7-month running mean) of SLP and surface winds for the antecedent phase (June to August of year −1), onset phase (November to December of year −1), development phase (March to April of year 0), and transition phase (July and August of year 0) for the three pre-1977 events (1957, 1965, and 1972).

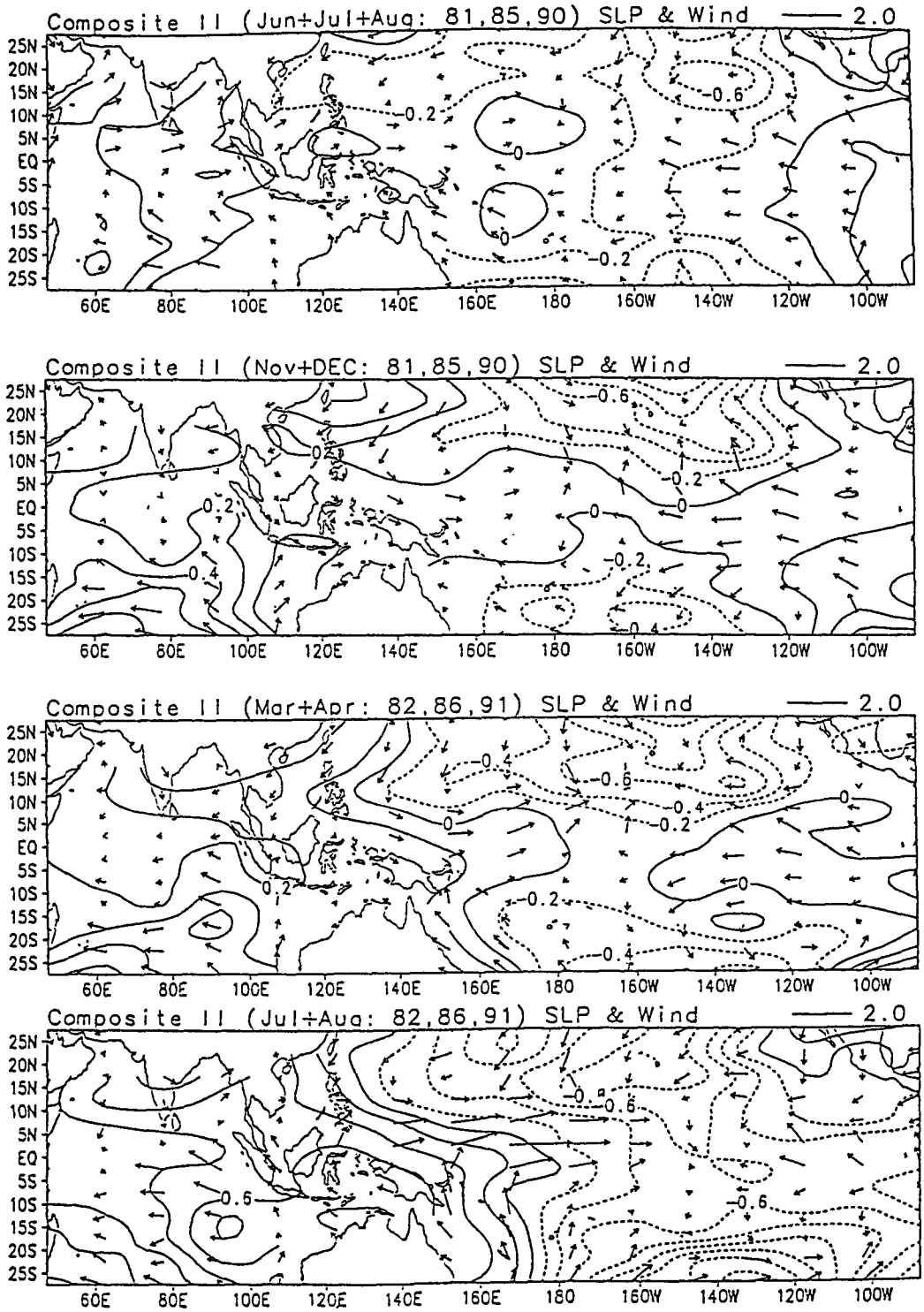

FIG. 7. As in Fig. 6 except for the three post-1977 events (1982, 1986–87, and 1991).

of the equator. These near-equatorial westerly anomalies are associated with a cyclonic gyre in the Philippine Sea that intensifies in situ from the antecedent to development phase (Figs. 7a–c). The establishment of the equatorial westerly anomalies in the western Pacific is, therefore, attributed to the development of the *Philippine Sea onset cyclone.* The intensification of the onset cyclone may be associated with the anomalous East

Asian winter monsoon in the 1982–83 and 1991 episodes but not in the 1986–87 episode. Persistent enhanced northeast monsoons can be seen in the northwestern Pacific behind the pressure trough (Figs. 7b,c).

From the onset to development phase, the composite atmospheric circulation anomalies for the pre-1977 warm episodes changed dramatically (Figs. 6b,c). The pressure rapidly decreased in the eastern Pacific and increased over the Maritime Continent. The equatorial easterly anomalies and accompanying divergence in the central Pacific suddenly disappeared and equatorial westerly anomalies were established in the entire western Pacific. On the contrary, the atmospheric anomalies of the post-1977 episodes changed steadily from the onset to development phase (Figs. 7b,c). The anomalous subtropical lows in the western North and South Pacific extended slightly eastward. The quasi-zonal pressure trough over the Philippine Sea deepened and the pressure trough over the SPCZ developed. Meanwhile, the pressure over Indonesia rose and the equatorial westerlies further strengthened.

In the transition phase the pre- and post-1977 composite SLP and surface anomalies display a similar pattern in the western-central Pacific (Figs. 6d and 7d). A common feature during the transition phase for both pre- and post-1977 warm episodes is the equatorial westerlies (easterlies) that are directed from the high anomalous SLP near 120°E to low SLP near 140°W (80°E). The slow eastward propagation of the equatorial westerly anomalies from the far western Pacific to the central Pacific is a common characteristic for all El Niño episodes in the last four decades.

b. SST anomalies

What causes the remarkable differences in the onset of atmospheric anomalies between the pre- and post-1977 El Niño episodes? To address this question the SST anomaly patterns for each of the six strong episodes were examined. Figures 8 and 9 present composite SST along with surface wind anomalies from the antecedent to transition phases for the pre- and post-1977 episodes, respectively.

As we noticed from Fig. 3a, the pre-1977 warm episodes were preceded by a strong (1956 and 1971) or a moderately strong (1964) cold event, whereas the post-1977 warm episodes were preceded by either a weak cooling (1981, 1985) or no cooling (1990) in year −1. This difference can be clearly observed from the composite SST anomalies in the antecedent and onset phases (Figs. 8a,b and 9a,b). In response to the strong negative SST anomalies in the central Pacific in the pre-1977 composite, surface winds diverged with notable easterly anomalies over the central and western Pacific and westerly anomalies in the eastern Pacific (Figs. 8a,b). In the post-1977 composite, on the other hand, the wind anomalies over the central and western equatorial Pacific are weak in accord with the weak equatorial SST gradients (Figs. 9a,b). The differences in the equatorial SLP and surface wind fields in the onset phase appear to be attributed to the differences in SST anomalies.

Another notable difference in SST anomalies is the location of major anomalous warming. For the pre-1977 composite, positive SST anomalies in the antecedent and onset phases occurred in the northern Australia and the SPCZ (Figs. 8a,b). There are large SST gradients between the equatorial cool water and the warm water in the SPCZ. The SST gradients would induce pressure gradients in the boundary layer via vertical turbulent transport of surface heat fluxes and hydrostatic balance (Lindzen and Nigam 1987). Near the equator the pressure gradient force approximately balances boundary layer friction, thus the winds blow down-pressure gradient from cold to warm water (across the anomalous SST "front"). Away from the equator, the Coriolis force tends to balance the pressure gradient force and boundary layer friction, turning wind anticlockwise, resulting in a northwesterly component along the SPCZ. That would favor the southeastward extension of the Australian cyclone. Conversely, for the post-1977 composite, major positive SST anomalies were located in an elongated area from the western equatorial Pacific to Baja California with a maximum occurring at (20°N and 140°W) (Figs. 9a,b). The positive SST anomalies in the western equatorial Pacific reach about one-half degree, which is significant because the annual and interannual variability of SST in that region is small. These positive SST anomalies persisted through the entire onset and development period and the corresponding SST gradients poleward of positive SST anomalies were enhanced from antecedent to onset phase (Figs. 9a–c). The SST anomalies in the central equatorial Pacific favor the development of anomalous westerlies along and slightly north of the equator and the formation of the cyclonic vorticity over the Philippine Sea.

5. Causes of the change in El Niño onset

The above observational evidence suggests that the fundamental differences in the Pacific Walker circulation, the off-equatorial onset cyclones, and the trades of the southeast Pacific in the onset phase result from the SST anomalies "memorized" by the ocean. Because the onset phase corresponds to a general transition from a cold (or on occasion from a near-neutral condition) to a warm state of the ENSO cycle, the SST anomalies associated with the ENSO cycle in this phase should be very small. What, then, accounts for the differences in the SST anomalies in the onset phase between the pre- and post-1977 warm episodes? One possible cause is that the background state, on which the ENSO cycle evolves, has secular variations on a timescale much longer than the ENSO timescale.

To test this idea, an empirical orthogonal function (EOF) analysis of secular SST variations on multide-

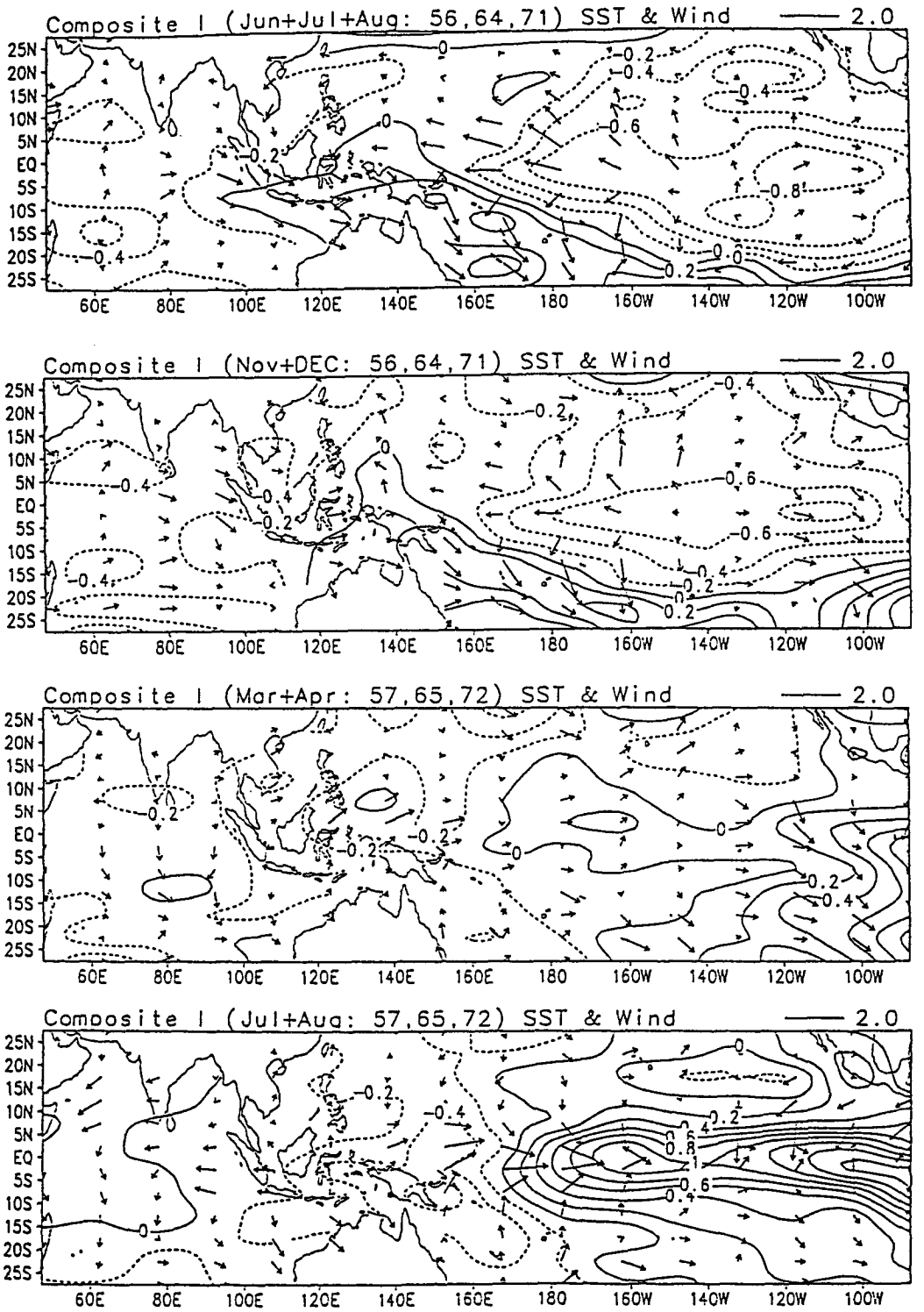

FIG. 8. As in Fig. 6 except for SST and surface wind anomalies.

cade timescale was performed. Although it is impossible to precisely define a "basic state" on which ENSO evolves due to the nonlinear feedback of the ENSO variability to the basic state, the SST variation on multidecade timescale may be studied by filtering out the ENSO variation from the monthly mean anomalies.

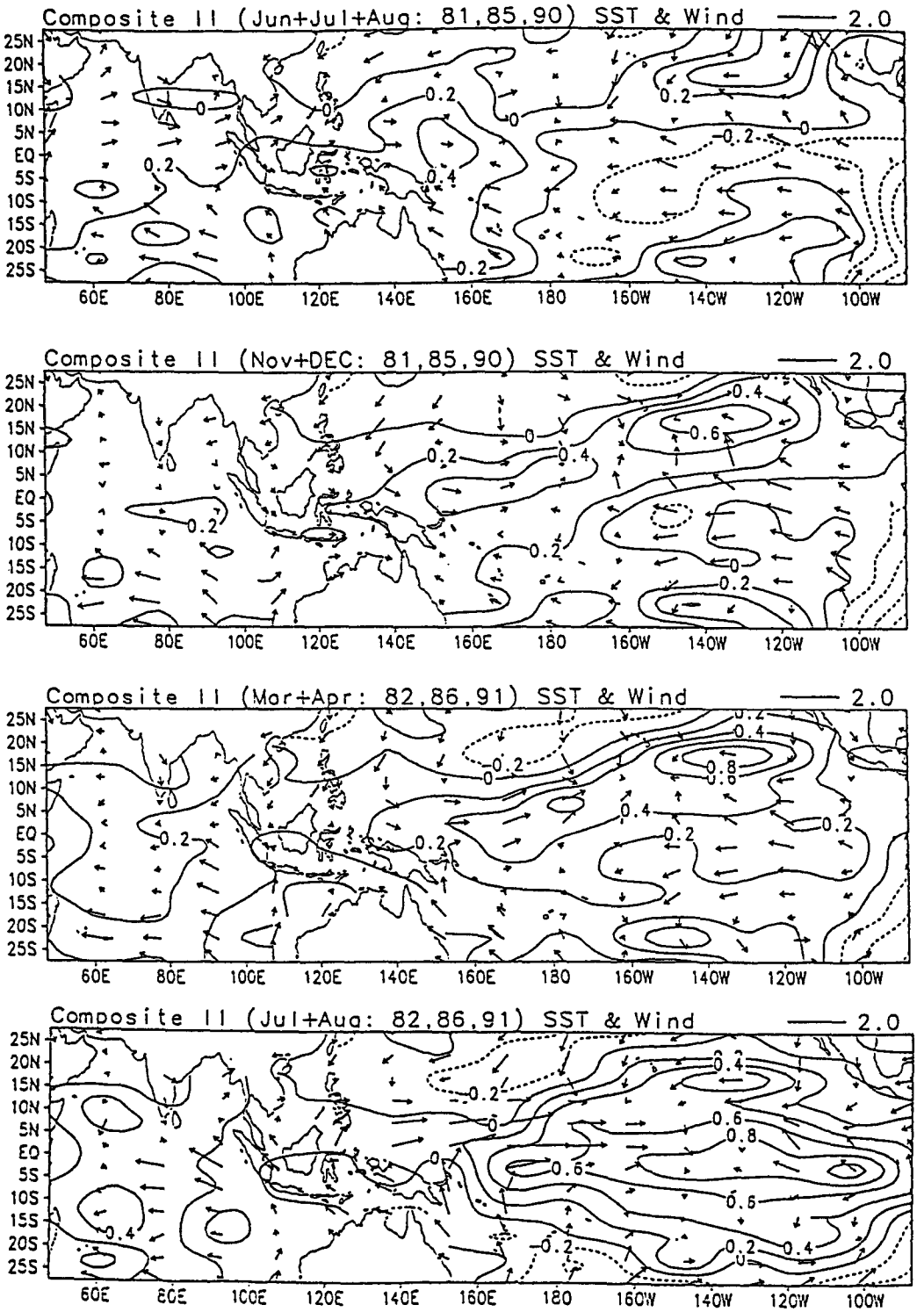

FIG. 9. As in Fig. 7 except for SST and surface wind anomalies.

A so-called interdecadal component was derived by a low-pass Sharpiro (1970) filtering of original 43-yr MMA series (which is similar to a 7-yr running mean MMA). Since the data quality in the early part of the 1950s is relatively poor, only the data from January 1958 to December of 1992 were used. Because the

temporal variation in the first and last three years was affected by the end effect of the applied filter, the principal component was displayed only for the period January 1961–December 1989 in Fig. 10. The most significant eigenmode accounts for about 62% of the variance of the interdecadal component. For a comparison, the total variance over the studied domain has also been computed for the 5-month running mean MMA of SST, which contains variations of both the ENSO and interdecadal components. The result shows that the ratio of the interdecadal variance to ENSO variance averaged over the entire domain is 32%, indicating that the first EOF mode of the interdecadal component has considerable contribution to the variance of low-frequency (interannual and interdecadal) variations.

The dominant interdecadal EOF mode shows two (a cold and a warm) quasi-steady phases and a relatively rapid transition from the cold to the warm state in the late 1970s over almost the entire tropical Pacific–Indian Ocean between 20°S and 20°N (Fig. 10). The strongest warming after the late 1970s occurs in the northeast Pacific around 120°W and 20°N and southeast Pacific around 120°W and 15°S. Another warming center is in the equatorial Pacific near the date line.

In the tropical Pacific, the spatial structure of the first EOF mode shown in Fig. 10 is remarkably similar to the difference in 10-year mean SST between the periods of 1977–1986 and 1967–1976 shown by Fig. 2 of Nitta and Yamada (1989). The latter was called an interdecadal variation. The interdecadal SST variation, however, is not confined to the Tropics, rather it is a basin-wide phenomenon. Accompanying the warming in the tropical areas between 20°S and 20°N, equally significant cooling takes place in the midlatitudes of both the North and South Pacific centered around 160°W (Nitta and Yamada 1989). In the North Pacific, the cooling after 1976 occurred in the central region (30°–50°N, 150°E–140°W) and approximately coincidental warming in the eastern region along the North American coast (Graham 1992).

The interdecadal SST anomalies appear to be coupled with interdecadal atmospheric circulation anomalies. Concurrent with the tropical warming after 1977, the convection over the west-central equatorial Pacific increased (Nitta and Yamada 1989; Graham 1992). The 500-hPa geopotential height in the northern midlatitudes in winter had lowered considerably during 1977–1986 (Kahiwabara 1987). The Pacific mean SLP for the winter period, November–March, averaged over

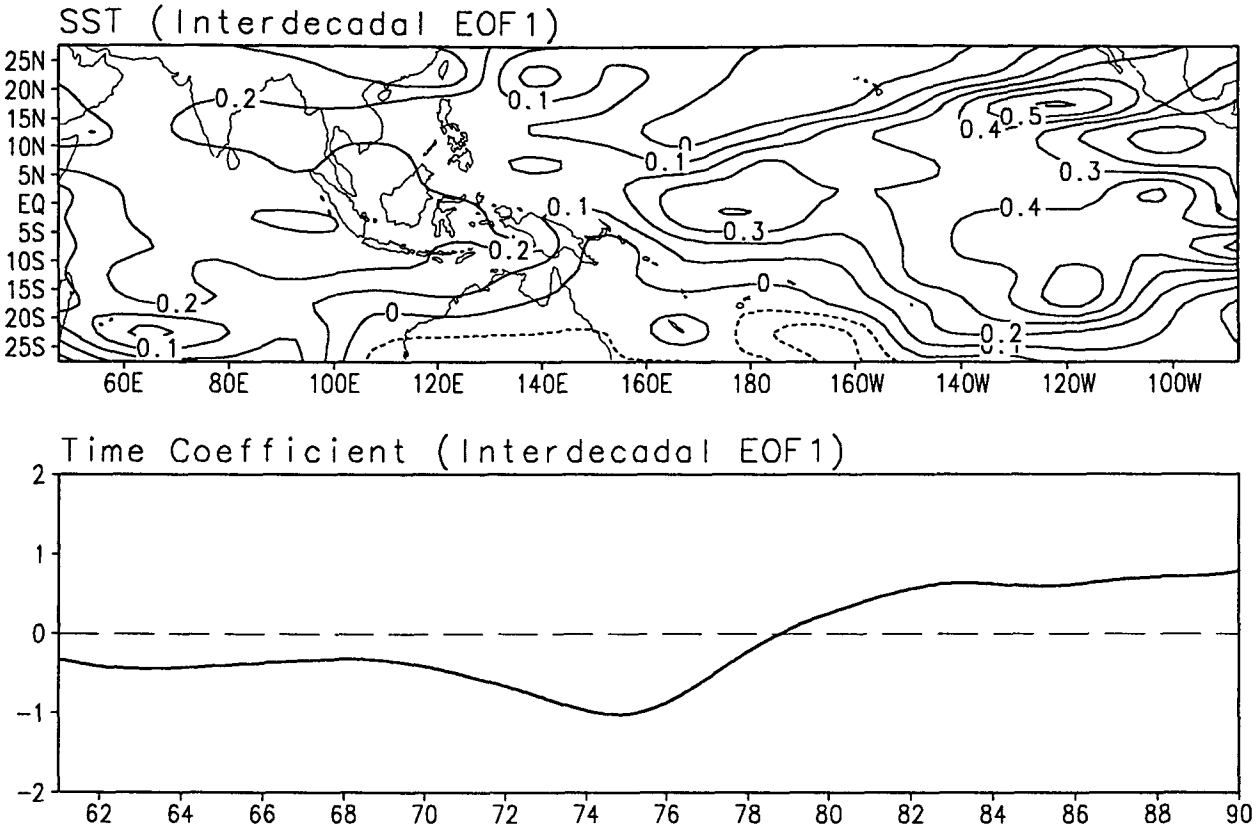

FIG. 10. (a) The spatial pattern and (b) temporal coefficient of the most important EOF mode of the interdecadal component of monthly mean SST anomalies.

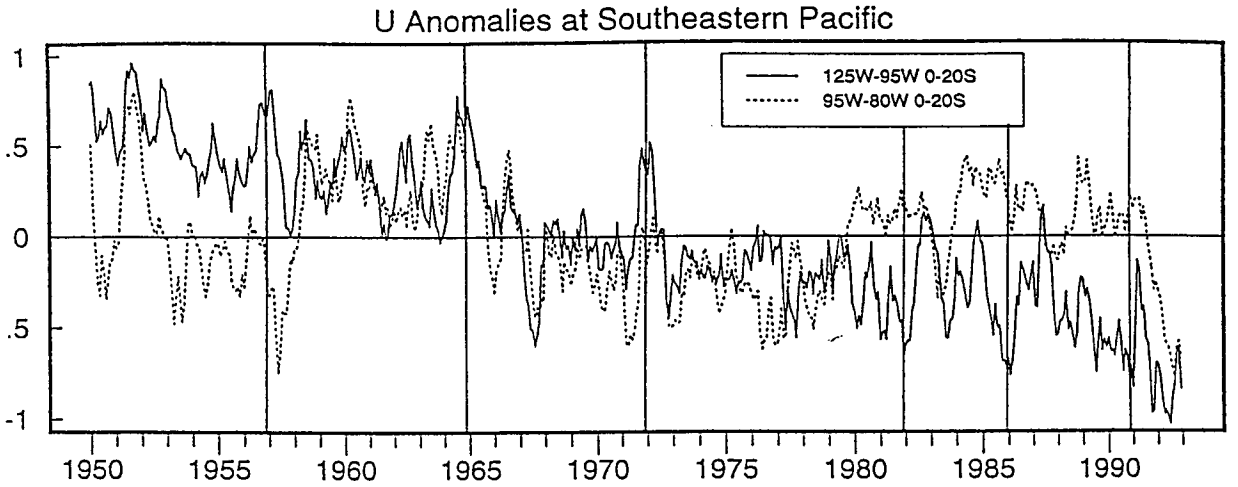

FIG. 11. Seven-month running mean westerly anomalies averaged over the open ocean (0°–20°S, 125°–95°W) and near the South American coast (0°–20°S, 95°–80°W) of the southeastern Pacific. Vertical lines indicate the December of the year preceding the six most significant El Niño events (1957, 1965, 1972, 1982, 1986–87, and 1991).

27.5°–72.5°N, 147.5°E–122.5°W, was lower by 2 hPa during 1977–1988 compared with the period 1946–1976 (Trenberth 1990). The Aleutian low was intensified and shifted southward with stronger than normal winter monsoons (Namias et al. 1988). Stronger westerlies occurred from 25°–45°N and weakened trades in the central Pacific (Inoue and O'Brien 1987). The North Pacific mean SLP is also an index of the Pacific–North American (PNA) teleconnection pattern (Wallace and Gutzler 1981) on the ENSO timescale (Trenberth 1990). In theory, the atmospheric response to anomalous tropical heating on an interdecadal timescale during northern winter should invoke similar mechanisms as those on the ENSO timescale that were suggested by Hoskins and Karoly (1981) and Simmons et al. (1983). However, the tropical interdecadal warming differs from a mature-phase El Niño in both the spatial distribution and strength. The excitation of inherent extratropical modes is expected to be different. Differences in the ENSO and interdecadal teleconnections were emphasized by Yamagata and Masumoto (1992).

The interdecadal changes in atmospheric circulations may, in turn, feed back to the ocean. The deepening of the Aleutian low would cause an anomalous cyclonic circulation over the North Pacific. This anomalous cyclone, on the one hand, may increase cold advection, evaporation, and ocean mixing west and south of the Aleutian low, leading to a cooling in the western and central North Pacific (Trenberth 1990); on the other hand, it may increase onshore Ekman transport along the west coast of North America, thereby suppressing upwelling and inducing anomalous warming. The increased wind curl associated with the enhanced westerlies south of the Aleutian low would also increase southward Sverdrup transport and accelerate the anticyclonic subtropical ocean gyre, favoring the formation of the positive SST anomalies stretching southwestward from Baja California to the central equatorial Pacific. The weakening of trades in the central Pacific would further enhance the warming there due to reduction in surface latent heat loss.

The change of El Niño onset in the late 1970s was concurrent with the above-described abrupt interdecadal change from a cold to a warm state. In fact, the composite SST anomalies in the onset phase for the pre- and post-1977 El Niño episodes are quite similar to the cold and warm states of the interdecadal mode, respectively (Figs. 8b, 9b, and 10). This implies that during the onset phase of El Niño, the background SST is, to a large degree, determined by the secular variation on longer timescales such as the sudden interdecadal change that occurred in the late 1970s.

Figure 11 shows zonal wind anomalies averaged along the South American coast (0°–20°S, 80°–95°W) and over a large area of the open ocean of the southeastern Pacific (0°–20°S, 95°–125°W). The data density in these regions is, on average, about 60 observations per month at each 5° lat by 15° long box (Fig. 1). The wind variation along the coast distinguishes from that over the open ocean of the southeast Pacific. There is an increasing trend in the strength of the trades over the open ocean of the southeast Pacific as evidenced by the decreasing trend of the corresponding westerly anomalies. There is no such trend in the southeast trades along the South American coast. Let us focus on the onset phase, that is, December of the year preceding the El Niño. The zonal wind anomalies near the coast have no definite relation with the coastal warming as noticed by Wyrtki (1975). The easterlies over the open ocean of the southeast Pacific, however, were significantly weaker than normal in the pre-1977

events, whereas they were significantly stronger than normal in the post-1977 episodes. This is consistent with the composite wind anomalies shown in Figs. 6b and 7b. Correspondingly, the South American coastal warming occurred in the development phase of the El Niño in the pre-1977 episodes, whereas it occurred after the mature phase in the post-1977 events (Fig. 3). It is believed that in the pre- (post-) 1977 episodes, the presence (absence) of coastal warming that precedes the central Pacific warming is a result of the positive feedback between the ocean and the relaxation (enhancement) of the trades in the southeast Pacific (0°–20°S, 95°–125°W). The relaxation of the trades over the open ocean of the southeast Pacific may effectively spindown the subtropical gyre, leading to a coastal warming in the development phase. The precise oceanic processes responsible for this remote response can be determined through numerical experiments.

6. Summary and discussion

In the onset phase of El Niño, the states of the atmosphere and ocean are close to their annual cycles. The coupling of the atmosphere and ocean is relatively weak because the annual cycle, to a large extent, is determined by insolational forcing, especially in the western Pacific. Even in the tropical eastern Pacific where air–sea interaction is involved, the insolational forcing also fundamentally regulates the annual cycle (Mitchell and Wallace 1992; Wang 1994a). As such, in the onset phase the interdecadal variations of the background state may effectively influence the evolution of the ENSO cycle.

It is hypothesized that the interdecadal change of the background state that occurred in the late 1970s is responsible for the changes in the characteristic evolution of the El Niño onset. The hypothesis is based on the evidence that the composite SST anomalies in the antecedent and onset phases for the pre- and post-1977 events (Figs. 8a,b and 9a,b) resemble, respectively, the cold and warm stages of the interdecadal variation in the tropical Pacific (Fig. 10). The hypothesis is also based on the assertion that the warm events evolving from a warm state of the interdecadal mode display features of onset that differ from those of the warm events evolving from a cold state of the interdecadal mode.

The processes by which the interdecadal mode possibly affects the onset of El Niño episodes are schematically summarized in Fig. 12. The warm state of the interdecadal mode that occurred after the late 1970s may influence the ENSO onset in two ways. First, the warming in the equatorial central Pacific and off-equatorial tropical eastern Pacific can offset the La Niña (cold episode) condition of an ENSO cycle in the antecedent phase, yielding a near-normal Walker circulation over the western and central Pacific and enhanced trades in the southeastern Pacific. The persistence of the enhanced southeast trades in the onset phase may prohibit South American coastal warming in the development phase, resulting in an absence of the coastal warming in boreal spring of the ENSO year that otherwise could lead the central Pacific warming. Another role of the interdecadal warming near the date line is to raise the mean SST, so that the SST along the equator would reach a given temperature (say 28°C) further east. This would favor eastward movements of convection and associated westerly anomalies from the western to central Pacific, leading to a central Pacific warming followed by a coastal warming in the year subsequent to the ENSO year. Second, the cooling in the western North Pacific favors a southeastward extension of east Asian winter monsoons so that northeasterly anomalies prevail north of the Philippine Sea. The large SST gradients on the poleward side of the interdecadal warming in the North Pacific would induce anomalous southwest thermal winds, which, together with the enhanced northeasterly monsoon, favor the formation of the Philippine Sea onset cyclone. After the late 1970s, the equatorial westerly anomalies, which eventually cause the Pacific warming, are associated with the development of this onset cyclone. Parallel arguments can be made as to how a cold state of an interdecadal variation could affect the background SST so that the coastal warming may lead the central Pacific warming and the formation of the Australia–SPCZ onset cyclone is favored.

The results derived from the present analysis suggest that secular changes in the background "mean" state may have profound impacts on the ENSO evolution. The anomaly models that are used to predict ENSO should take into account this factor in specification of the model's mean states.

In addition to the interdecadal mode, relatively high-frequency (intraseasonal to annual timescales) disturbances, perhaps primarily in the extratropical atmosphere, could also interfere with the ENSO mode and cause irregularities in the ENSO cycle. The occurrence of minimum pressure anomalies during the onset phase in the subtropics around the node line of the Southern Oscillation (15°–30°N and 15°–30°S, 160°E–155°W), especially in the North Pacific subtropics (Figs. 5b and 6b), may be related to abnormal seasonal variations in the extratropical atmosphere. This pressure fall favors the establishment of the onset cyclones and the equatorial westerly anomalies over the western Pacific, which play a critical role in the initiation of the instability of the coupled ocean/atmosphere system in the western-central Pacific. The common features of the transition from a cold to a warm state of the ENSO cycle have been discussed in detail in an accompanying paper (Wang 1994b). The exact cause of the pressure fall near the node line of the Southern Oscillation before and during the onset phase of El Niño is not clear and calls for further investigations.

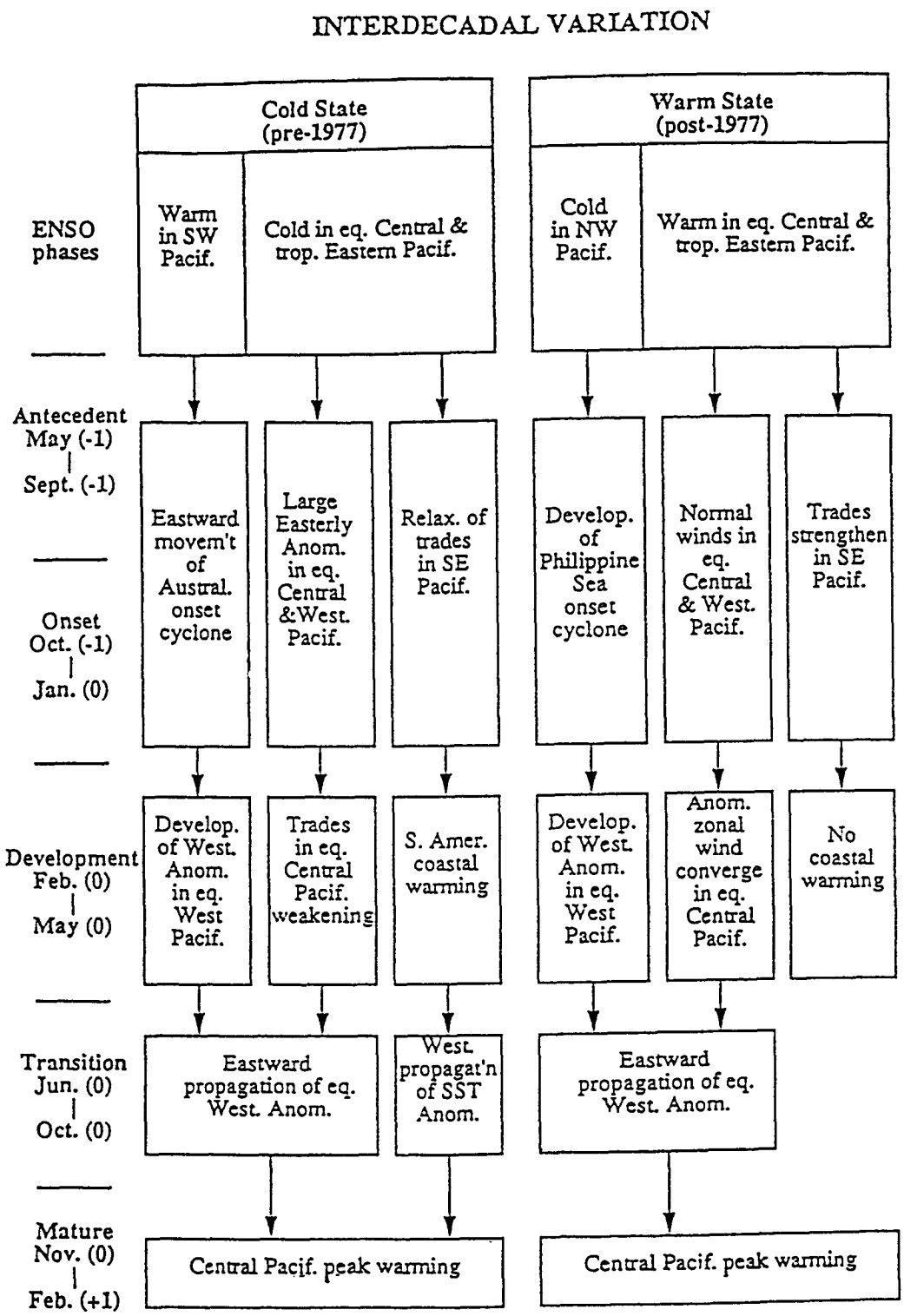

FIG. 12. Schematic diagram showing the impacts of the interdecadal variation on the ENSO onset.

There is a possible feedback from ENSO episodes to the interdecadal variations. However, the fact that the interdecadal mode has a different spatial pattern from the ENSO mode and the interdecadal change of phase occurred before the extremely strong 1982 ENSO appears to suggest it is unlikely that the interdecadal SST change resulted from the excessive intensity of recent warm episodes. It is not known, however, what causes the relatively abrupt interdecadal change and what maintains the interdecadal SST anomalies. Further studies of the interaction between ENSO and interdecadal variation and the teleconnections between the Tropics and midlatitudes of both hemispheres on both interdecadal and ENSO timescales are necessary to reveal the cause of the interdecadal variation and to further assess its impact on the evolution of ENSO.

Acknowledgments. The author thanks Yan Wang, Yuxiang He, and Debra Kessler for their technical assistance. The revision of the manuscript benefited from comments by anonymous reviewers, T. Murakami, A. J. Wagner, R. E. Livezey, and J. J. O'Brien, and discussions with C. Ropelewski and J. von Storch. This research was supported by the NOAA EPOCS program. This is the School of Ocean and Earth Science and Technology publication number 3662.

REFERENCES

Barnett, T. P., 1983: Interaction of the monsoon and Pacific trade wind systems at interannual time scales. Part I: The equatorial zone. *Mon. Wea. Rev.*, **111,** 756–773.

——, 1984: Interaction of the monsoon and Pacific trade wind system at interannual time scales. Part III: A partial anatomy of the Southern Oscillation. *Mon. Wea. Rev.*, **112,** 2388–2400.

——, 1985: Variations in near global sea level pressure. *J. Atmos. Sci.*, **42,** 478–501.

Bjerknes, J., 1966: A possible response of the atmospheric Hadley circulation to equatorial anomalies of ocean temperature. *Tellus.* **18,** 820–829.

——, 1969: Atmospheric teleconnections from the equatorial Pacific. *Mon. Wea. Rev.*, **97,** 163–172.

Busalacchi, A., and J. J. O'Brien, 1981: Interannual variability of the equatorial Pacific in the 1960's. *J. Geophys. Res.*, **86,** 10 901–10 907.

Cane, A. M., 1993: Tropical Pacific ENSO models: ENSO as a mode of the coupled system. *Climate System Modeling.* K. E. Trenberth, Ed., Cambridge University Press, 788 pp.

Desser, C., and J. M. Wallace, 1987: El Niño events and their relation to the Southern Oscillation: 1925–1986. *J. Geophys. Res.*, **92,** 14 189–14 196.

——, and ——, 1990: Large-scale circulation features of warm and cold episodes in the tropical Pacific. *J. Climate,* **3,** 1254–1281.

Gill, A. E., and E. M. Rasmusson, 1983: The 1982–83 climate anomaly in the equatorial Pacific. *Nature,* **306,** 229–234.

Graham, N. E., 1992: Decadal scale climate variability in the 1970s and 1980s: Observations and model results. *Decadal-to-Century Time Scales of Climate Variability.* Academic Press.

Gutzler, D. S., and D. E. Harrison, 1987: The structure and evolution of seasonal wind anomalies over the near-equatorial eastern Indian and western Pacific Oceans. *Mon. Wea. Rev.*, **115,** 169–192.

Hackert, E. C., and S. Hastenrath, 1986: Mechanisms of Java rainfall anomalies. *Mon. Wea. Rev.*, **114,** 745–757.

Horel, J. D., and J. M. Wallace, 1981: Planetary-scale atmospheric phenomena associated with the Southern Oscillation. *Mon. Wea. Rev.*, **109,** 813–829.

Hoskins, B. J., and D. J. Karoly, 1981: The steady linear response of a spherical atmosphere in thermal and orographical forcing. *J. Atmos. Sci.*, **38,** 1179–1196.

Inoue, M., and J. J. O'Brien, 1987: Trends in sea level in the western and central equatorial Pacific during 1974–75 to 1981. *J. Geophys. Res.*, **92**(C5), 5045–5051.

Janowiak, J. E., 1993: Seasonal climate summary: The global climate for September–November 1991: Warm (ENSO) episode conditions strengthen. *J. Climate,* **6,** 1616–1638.

Kahiwabara, T., 1987: On the recent winter cooling in the North Pacific (in Japanese). *Tenki,* **34,** 777–781.

Keen, R. A., 1982: The role of cross-equatorial cyclone pairs in the Southern Oscillation. *Mon. Wea. Rev.*, **110,** 1405–1416.

Kiladis, G. N., and H. van Loon, 1988: The Southern Oscillation. Part VII: Meteorological anomalies over the Indian and Pacific sectors associated with the extremes of the oscillation. *Mon. Wea. Rev.*, **116,** 120–136.

Kousky, V. E., 1993: Seasonal Climate Summary: The global climate of December 1991–February 1992: Mature phase warm (ENSO) episode conditions develop. *J. Climate,* **6,** 1639–1655.

——, and A. Leetmaa, 1989: The 1986–87 Pacific warm episode: Evolution of oceanic and atmospheric anomaly fields. *J. Climate,* **2,** 254–267.

Lau, K. M., and P. H. Chan, 1983: Aspects of the 40–50 day oscillation during the northern summer as inferred from outgoing longwave radiation. *Mon. Wea. Rev.*, **114,** 1354–1367.

——, C.-P. Chang, and P. H. Chan, 1986: Short-term planetary-scale interactions over the Tropics and midlatitudes. Part II: Winter MONEX period. *Mon. Wea. Rev.*, **111,** 1372–1388.

Lindzen, R. S., and S. Nigam, 1987: On the role of sea surface temperature gradients in forcing low-level winds and convergence in the Tropics. *J. Atmos. Sci.*, **45,** 2440–2458.

Meehl, G. A., 1987: The annual cycle and interannual variability in the tropical Pacific and Indian Ocean region. *Mon. Wea. Rev.*, **115,** 27–50.

Mitchell, T. P., and J. M. Wallace, 1992: The annual cycle in equatorial convection and sea surface temperature. *J. Climate,* **5,** 1140–1156.

Namias, J., X. Yuan, and D. R. Cayan, 1988: Persistence of North Pacific sea surface temperature and atmospheric flow patterns. *J. Climate,* **1,** 682–703.

Nitta, T., and S. Yamada, 1989: Recent warming of tropical surface temperature and its relationship to the Northern Hemisphere circulation. *J. Meteor. Soc. Japan,* **67,** 375–383.

Philander, S. G., 1981: The response of equatorial oceans to a relaxation of the trade winds. *J. Phys. Oceanogr.*, **11,** 176–189.

——, 1985: El Niño and La Niña. *J. Atmos. Sci.*, **42,** 2652–2662.

——, and E. M. Rasmusson, 1985: The Southern Oscillation and El Niño. *Adv. Geophys.*, **28,** 197–215.

Rasmusson, E. M., and T. H. Carpenter, 1982: Variations in tropical sea surface temperature and surface wind fields associated with the Southern Oscillation/El Niño. *Mon. Wea. Rev.*, **110,** 354–384.

Shapiro, R., 1970: Smoothing, filtering, and Boundary effects. *Rev. Geophys. Space Phys.*, **8,** 359–387.

Simmons, A. J., J. M. Wallace, and G. W. Branstator, 1983: Barotropic wave propagation and instability, and atmospheric teleconnection patterns. *J. Atmos. Sci.*, **40,** 1363–1392.

Trenberth, K. E., 1990: Recent observed interdecadal climate changes in the Northern Hemisphere. *Bull. Amer. Meteor. Soc.*, **71,** 988–993.

——, and D. J. Shea, 1987: On the evolution of the Southern Oscillation. *Mon. Wea. Rev.*, **115,** 3078–3096.

van Loon, H., and D. J. Shea, 1985: The Southern Oscillation. Part IV: The precursors south of 15°S to the extremes of the oscillation *Mon. Wea. Rev.*, **113,** 2063–2074.

——, and ——, 1987: The Southern Oscillation. Part VI: Anomalies of sea level pressure on the Southern Hemisphere and of Pacific

sea surface temperature during the development of warm event. *Mon. Wea. Rev.*, **115,** 370–379.

Wallace, J. M., and D. S. Gutzler, 1981: Teleconnections in the geopotential height during the Northern Hemisphere winter. *Mon. Wea. Rev.*, **109,** 784–812.

Wang, B., 1992: The vertical structure and development of the ENSO anomaly mode during 1979–1989. *J. Atmos. Sci.*, **49,** 698–712.

——, 1994a: On the annual cycle in the tropical eastern-central Pacific. *J. Climate,* **7,** 1926–1942.

——, 1994b: Transition from a cold to a warm state of the El Niño–Southern Oscillation cycle. *Meteor. Atmos. Phys.*, in press.

Woodruff, S. D., R. J. Sultz, R. L. Jenne, and P. M. Steurer, 1987: A comprehensive ocean–atmosphere data set. *Bull. Amer. Meteor. Soc.*, **68,** 1239–1250.

Wyrtki, K., 1975: El Niño—The dynamic response of the equatorial Pacific Ocean to atmospheric forcing. *J. Phys. Oceanogr.*, **5,** 572–584.

——, 1982: The Southern Oscillation, ocean–atmosphere interaction and El Niño. *Mar. Tech. Soc. J.*, **16,** 3–10.

Yamagata, T., and Y. Masumoto, 1992: Interdecadal natural climate variability in the western Pacific and its implication in global warming. *J. Meteor. Soc. Japan,* **70,** 167–175.

Yasunari, T., 1985: Zonally propagating modes of the global west circulation associated with the Southern Oscillation. *J. Meteor. Soc. Japan.* **63,** 1013–1029.

——, 1990: Impact of Indian monsoon on the coupled atmosphere/ocean system in the tropical Pacific. *Meteor. Atmos. Phys.*, **44,** 29–41.